Computers and Electrical Engineering 60 (2017) 161–174

Contents lists available at ScienceDirect

Computers and Electrical Engineering

journal homepage: www.elsevier.com/locate/compeleceng

Beam pattern synthesis based on improved biogeography-based optimization for reducing sidelobe level☆

Han Li[a], Yanheng Liu[a,b], Geng Sun[a,d,*], Aimin Wang[a,b,*], Shuang Liang[c]

[a] College of Computer Science and Technology, Jilin University. Changchun, Jilin 130012, China
[b] Key Laboratory of Symbolic Computation and Knowledge Engineering of Ministry of Education, Jilin University, Changchun, 130012, China
[c] College of Software, Jilin University, Changchun, Jilin 130012, China
[d] School of Electrical and Computer Engineering, Georgia Institute of Technology, Atlanta, 30332, USA

ARTICLE INFO

Article history:
Received 6 May 2016
Revised 3 January 2017
Accepted 4 January 2017
Available online 10 January 2017

Keywords:
Antenna array
Biogeography-based optimization
Sidelobe level
Radiation beam pattern

ABSTRACT

This study deals with a design problem of linear and circular antenna arrays (LAAs and CAAs, respectively) for suppressing the sidelobe levels (SLLs). By adding a new local search strategy and a selection operator into the normal biogeography-based optimization, this work develops a biogeography-based optimization based on local search (BBOLS) algorithm to determine an optimal set of excitation current values for LAAs and an optimal set of excitation current as well as spacing values for CAAs. Various simulations are performed to examine the effectiveness of the proposed BBOLS algorithm in optimizing the radiation beam patterns of LAAs and CAAs, and the results show that BBOLS algorithm has a better performance in reducing the maximum SLL compared with other algorithms such as firefly algorithm.

1. Introduction

Antenna arrays play an important role in modern wireless communications, especially in mobile communications, satellite communications, and radar systems. Given the rapid development of the fourth generation (4 G) communication systems, researchers across the world have begun to focus on the fifth generation (5 G) cellular networks, which are known for their high density, self-organization, massive antenna arrays, multi-carriers based on filter banks and full duplex reuse. With the exponential increase in the volume of data traffic, the millimeter-wave (mm-wave) spectrum technology which can provide channels with large bandwidths is adopted in the 5 G wireless communication systems [1]. Moreover, in order to fully utilize the spectrum resources generated by the mm-wave spectrum technology, the massive multi-input-multi-output (MIMO) technology with high spectral efficiency has been proposed [2,3]. Space division multiple access (SDMA) is an important practical example of the massive MIMO technologies in 5 G communication systems, and it can make the electromagnetic wave propagate to a certain direction so that reducing the cost of the transmission energy.

The technology of propagating the electromagnetic wave in a specific direction is called beamforming which can be generated by antenna arrays. In addition, even though the licensed spectrums are the basic resources of 5 G communication systems, the unlicensed spectrums are being expanded to use to build a network with higher speed, lower latency and less electricity consumption. This will also meet the needs of link demands for the huge number of devices in the Internet

☆ Reviews processed and recommended for publication to the Editor-in-Chief by Guest Editor Dr. P. Nagaradjane.

* Corresponding author.
E-mail addresses: sungeng207@foxmail.com (G. Sun), wang_ai_min@126.com (A. Wang).

http://dx.doi.org/10.1016/j.compeleceng.2017.01.003

of things. Moreover, the communication range is an important property for 5 G communication systems, thus the antenna arrays can be used to improve the communication range of these communication systems efficiently. Antenna arrays can also be used to enhance the signal quality, the coverage area, the connectivity rate and the spectral efficiency of these systems [4]. With the fast development of the antenna arrays, it trends to involve incorporating higher frequency bands (including optical), larger bandwidth, larger power levels and higher gain with larger size, and then making possible to decrease the input impedance to the required level [5]. However, the radiation beam patterns of antenna arrays still have a decisive role in the performance of communication systems. The performance criteria of antenna arrays include beam width, sidelobe level (SLL), noise sensitivity, directivity and robustness. To evaluate the beam pattern performances of antenna arrays, this study considers a design criterion of minimum SLL by using an improved biogeography-based optimization (BBO) algorithm.

The rest of this paper is organized as follows. Section 2 introduces some prime existing achievements in the field of radiation beam pattern optimization problems. Section 3 discusses the geometry and array factors for both linear antenna arrays (LAAs) and circular antenna arrays (CAAs), and creates the fitness function based on these models. Section 4 introduces the proposed optimization method, while Section 5 presents its numerical results. Section 6 summarizes the findings and concludes the paper.

2. Related work

The techniques for designing antenna arrays are mainly focused on two classes that are the uniform spacing and the non-uniform spacing antenna arrays. The main difference of these two classes is that the uniform case is analytically tractable, and the non-uniform case can be only treated by numerical approximations. Moreover, the techniques for designing these two kinds of antenna arrays are usually based on the mathematical programming, such as constrained programming [6]. However, in recently years, some techniques based on the swarm intelligence approaches have been gradually used to the design of antenna arrays.

Zhang et al. propose a real-coded genetic algorithm (RGA) optimization method to optimize the weight of each antenna element to minimize the SLL of the uniform spacing LAA with a certain main beam width [7]. Florence et al. utilize the accelerated particle swarm optimization (PSO) algorithm to synthesize two classes of uniform spacing arrays that use unequal phases with equal and unequal amplitudes [8]. Singh, et al. use cuckoo optimization algorithm (COA) to determine a set of parameters of antenna elements that provides the required radiation beam patterns [9]. COA is a novel nature inspired computing algorithm which is motivated by the life of cuckoo, and it is also a population-based method. Pappula et al. propose a new evolutionary technique, named cat swarm optimization (CSO), for the synthesis of LAAs [10]. CSO has a better performance for solving linear and non-linear optimization problems, and it is also applied to optimize the antenna element positions for suppressing SLLs and for achieving nulls in desired directions. Swain et al. apply gravitational search algorithm (GSA) to linear dipole antenna array (LDAA) optimizations [11], and GSA is used to achieve narrow beam width and lower SLL for LDAA. Qubati et al. use the central force optimization algorithm into the optimal design of two wideband micro-strip patch antennas [12]. To synthesize thinned linear antenna arrays with low SLLs, Guney et al. introduce a method based on the bees algorithm, which is inspired by the behavior of the honeybees in finding an optimal way of harvesting food resources around the hive [13]. Ram et al. use the firefly algorithm (FA) to design non-uniform CAAs for minimum the SLLs and reducing the first null beam widths (FNBWs) [14]. This method is used to determine an optimal set of excitation weights as well as inter-element separations for optimizing the beam patterns and the FNBWs.

This study proposes a BBO based on local search (BBOLS) algorithm to optimize the radiation beam patterns of LAAs and CAAs. BBOLS improves the precision of the BBO algorithm by adding a local search strategy and a selection operator. For solving the multi-dimensional optimization problems, BBOLS can not only ensure the normal computational capabilities, but also reduce the convergence speed of BBO, thereby avoiding local convergence.

The main contributions of this paper are highlighted as follows.

(1) A novel BBOLS algorithm is introduced to the design of LAAs and CAAs for suppressing the sidelobe levels.
(2) The proposed BBOLS adds the local search strategy and selection operator into the original BBO algorithm. The differential evolution algorithm with a new local search strategy (DELSS) can increase the diversity of the population for BBO because of its randomness, parallelism and effective expansion. Moreover, the selection operator can make the final solution tend to the optimal location.
(3) According to the numerical results, the performance of BBOLS is better than normal BBO, FA and PSO in suppressing the SLLs of LAAs and CAAs.

3. System model

3.1. LAA

LAA is a kind of antenna arrays with the simplest fabrication and implementation. Fig. 1(a) shows an LAA model with $2N$ elements that are symmetrically distributed along the x axis. The array factor of an LAA is expressed as follows [15]:

$$AF(\phi) = \sum_{\substack{n=-N \\ n\neq 0}}^{N} I_n \exp(j[kx_n \cos(\phi) + \alpha_n]) \tag{1}$$

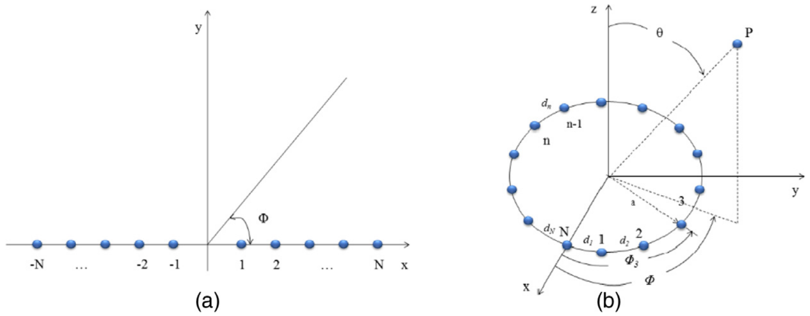

Fig. 1. Geometry of antenna array. (a) Geometry of 2*N*-element-symmetric LAA placed along the *x* axis; (b) Geometry of a non-uniform CAA with *N* isotropic antennas.

where k represents the wave number, I_n is the excitation amplitude of the nth element, α_n is the phase of the nth element, x_n is the location of the nth element and Φ is the azimuth angle measured from the positive x axis.

3.2. CAA

Fig. 1(b) shows the geometry of a CAA with N isotropic antenna elements that are non-uniformly placed on a ring with radius a lying on the x-y plane ($\theta = 90°$). These elements are assumed to be the isotropic radiators, and the array factor of a CAA is expressed as follows [15]:

$$AF(\theta, \phi) = \sum_{n=1}^{N} I_n \exp(j[ka\sin(\theta)\cos(\phi - \phi_n) + \alpha_n]) \tag{2}$$

$$ka = \frac{2\pi}{\lambda}a = \sum_{i=1}^{N} d_i \tag{3}$$

$$\phi_n = \frac{2\pi\sum_{i=1}^{n} d_i}{ka} \tag{4}$$

$$\alpha_n = -ka\sin(\theta_0)\cos(\phi_0 - \phi_n) \tag{5}$$

where I_n is the excitation amplitude of the nth element, α_n is the phase of the nth element, and d_n represents the arc separation between nth and (n–1)th elements, d_1 is the arc distance between the first ($n = 1$) and last ($n = N$) elements. Moreover, Φ_n represents the angular position of the nth element in the x–y plane, Φ is the azimuth angle measured from the positive x axis, θ is the elevation angle measured from the positive z axis, the array factor in this work is in the x–y plane ($\theta = 90°$), θ_0 and Φ_0 are set to be 90° and 0°, respectively (i.e., the peak of the main beam is directed along the positive x-axis).

3.3. Fitness function

This work aims to design antenna arrays with minimum SLLs. Therefore, the optimization problem is formulated as follows [16]:

$$\text{Minimize} \quad fitness = \max\left\{20\log_{10}\left|\frac{AF(\phi)}{AF(\phi_0)}\right|\right\} Subject\ to\ \phi \in [-\phi_n, \phi_n] \tag{6}$$

For the design of LAAs with minimum SLLs, Φ_n is assumed to be 90°, and the optimization process aims to optimize the current amplitude (I_n). For the design of CAAs with minimum SLLs, Φ_n is assumed to be 180°, and the optimization process aims to optimize the current amplitude (I_n) and the arc distance between the elements (d_n).

4. Methods

Reference [17] has illustrated that BBO has a better performance for solving multi-objective, global, and population-based optimization problems. It uses biogeography-based migration operator and mutation operator to share the information among the candidate solutions to increase the diversity of the population. Therefore, we try to use a BBO-based algorithm to optimize the beam pattern, and the effect of the BBO has been shown in Section 5.1.

Table 1
Pseudo-code of BBO.

BBO
1: Initialization
Initialize the BBO parameters: population size N, number of SIVs in an individual m, maximum number of generations Gen_{max}, maximum emigration rate E, maximum immigration rate I, elitism parameter $Keep$, maximum mutation rate m_{max}, and $gen = 0$.
Initialize the population: generate a random set of habitats P_0, and the population size is N.
2: Calculate the fitness value of each individual in P_0
3: Map the fitness values to the number of species S
Calculate the immigration rate λ and emigration rate μ for each individual in the population
4: Migration
Use immigration rate λ and emigration rate μ to modify the selected individual in the population, and then re-compute the fitness value for each individual.
5: Mutation
Mutate each non-elite individual based on its probability, and then re-compute the fitness value for each individual.
6: Stopping criteria
If $gen \geq Gen_{max}$ or an acceptable problem solution is found, then this loop can be terminated. Otherwise, if $gen = gen + 1$, proceed to step (3).

4.1. BBO

BBO is a global evolutionary multi-dimensional optimization method proposed by Simon in 2008 [17]. Biogeography studies the geographical distribution of biological organisms, whose migration behaviors govern their distributions. The mathematical model of BBO describes the migration and extinction of species between neighboring habitats, with each habitat being geographically isolated from other habitats. In some geographical areas, a habitat with a high habitat suitability index (HSI) is suitable for biological species. HSI can be influenced by rainfall, temperature, and other factors. These factors that influence HSI are called suitability index variables (SIVs).

Suppose one global optimization problem with several candidate solutions can be represented as an array that comprises SIVs. This array can be written as Habitat = [SIV_1, SIV_2, SIV_3, ..., SIV_m]. Then HSI can be expressed as follows: fitness(Habitat) = HSI = f(SIV_1, SIV_2, SIV_3, ..., SIV_m). Migration and mutation are employed to optimize the solutions of the optimization problem in BBO. Migration refers to the process of moving species from one habitat to another. A habitat with a mass of species has high HSI, high emigration rate, low immigration rate and highly stable construction. However, a habitat with only a handful of species shows the opposite characteristics. This migration process is identical to the changing of information between different solutions in the optimization problem, which in turn leads to information sharing among various solutions. In BBO, every solution corresponds to a mutation rate, and a solution with a high mutation rate will be changed into other solutions. This mutation mechanism increases the diversity of solutions for the optimization problem. Table 1 shows the pseudo-code of BBO.

4.2. Improved BBO

To acquire the global optimum solution, this study adds local search strategy into normal BBO to develop a novel BBOLS algorithm. The concrete modified tactics for BBO are characterized in two steps, namely, (1) adding the local search strategy into the migration, and (2) employing the selection operator for the population after using the migration and local search operators. In sum, BBOLS employs the combination of the migration and local search operators to optimize the population in each iteration, uses the selection operator to compare the fitness values for the individuals in the new population with those of the corresponding individuals in the old population, and keeps those individuals with higher fitness values to constitute a new population to the next iteration. The following sections discuss the improved migration operation, and the selection operation in detail.

4.2.1. Improved migration operation

The migration operation in BBO uses the immigration rate λ and emigration rate μ of each individual to determine which SIVs from those individuals with higher emigration rates must be immigrated into those individuals with higher immigration rates. As the iterations increase, the differences among these individuals will also diminish, and the convergence speed will reduce. These features increase the likelihood for the solutions of the optimization problem to be trapped into the local optimum. Therefore, DELSS [18] is incorporated into the migration operation in BBO to avoid immigrating some SIVs to those individuals with higher immigration rates and no use for these SIVs.

Suppose the current populations = {X_1, X_2,..., X_N}, where N represents the number of individuals in the whole population. Randomly selecting three individuals, $X_i = (x_1, x_2,..., x_m)$, $X_j = (x'_1, x'_2,..., x'_m)$, and $X_k = (x''_1, x''_2,..., x''_m)$, where $i \neq j \neq k$, and m is the number of variables for the individual. The new individual X' is generated as follows:

$$X'(w) = X_i(w) + R(-1, 1)(X_j(w) - X_k(w)), w = 1, 2, ..., m \tag{7}$$

where $R(-1,1)$ is an even-distributed random number which ranges between −1 and 1. Formula (7) is to make local climbing operation for current individual X, and the new generated individual X' will intersect with X.

Table 2
Pseudo-code of migration based on local search.

Local search
1: for $h = 1$: n do
2: randomly select three individuals X_i, X_j, and X_k, ($i \neq j \neq k$) from the whole population
3: utilize Formula (7) to generate a new individual X' according to X_i, X_j, and X_k
4: randomly select one position K from m variables
5: for $u = 1$: m do
6: if $rand < lambdaScale$
7: if $rand <= C$ || $u = K$ // If the generated random number is less than mutation probability C or // $u = K$, then copy the value of u^{th} variable in X' to $Island(h,u)$
8: $Island(h,u) = X'(u)$
9: else // including steps 10 to 17, if $RandomNum$ is less than $Select$, then assign the value of // u^{th} variable in the current individual to $Island(h,u)$
10: $RandomNum = rand$ * sum(mu)
11: $Select = mu(1)$
12: $SelectIndex = 1$
13: while($RandomNum > Select$) && ($SelectIndex < n$)
14: $SelectIndex = SelectIndex + 1$
15: $Select = Select + mu(SelectIndex)$
16: end while
17: $Island(h,u) = X_{SelectIndex}(u)$
18: end if
19: else
20: $Island(h,u) = X_h(u)$
21: end if
22: end for
23: end for

Table 3
Pseudo-code of selection operation.

Selection
1: for $h = 1$: n
2: if fitness($Island(h)$) $<$ fitness(X_h)
3: $X_h = Island(h)$
4: end if
5: end for

Table 2 shows the pseudo-code of migration based on local search. The newly generated population is located in the *Island*.

4.2.2. Selection operation

The population in the *Island* still demonstrates randomness after the migration. Therefore, the migration operation cannot guarantee that the individuals will proceed to the next iteration with higher HSIs. To achieve better performance, selection operation is applied to the populations after the migration operation. In this operation, the fitness values for the individuals in *Island*, which is generated after the migration operation, are compared with those of the corresponding individuals in the old population. Afterward, those individuals with higher fitness values are selected to compose the new population to the next iteration. Selection operation ensures that all best individuals from the current iteration will be transferred to the next iteration. Table 3 shows the pseudo-code of selection operation.

4.2.3. Main procedure of BBOLS

Table 4 shows the pseudo-code of BBOLS, and the main updating procedures of BBO and BBOLS are shown in Fig. 2(a) and Fig. 2(b), respectively. In Fig. 2(a), the first updating procedure for the individual H_i of BBO is that randomly selecting an individual H_j which is different from H_i; second, randomly selecting a number d from 1 to m, and then using the *SIV(j, d)* in H_j to replace *SIV(i, d)* in H_i to complete the migration operation; third, generating a random number *r1* and using the mutation rate to generate a number r from 1 to m, and then using *r1* to replace the *SIV(i, r)* in H_i to complete the mutation operation; finally, a new individual H_i is generated.

Moreover, in Fig. 2(b), the first updating procedure for the individual H_i of BBOLS is that randomly selecting four individual H_j, H_{j1}, H_{j2} and H_{j3} which are different from H_i; second, randomly selecting a number d from 1 to m, and then using the *SIV(j, d)* in H_j to replace *SIV(i, d)* in H_i to complete the migration operation; third, utilizing Formula (7) which contains H_{j1}, H_{j2} and H_{j3} to create H_{j4}, using the mutation rate to select a number h from 1 to m, and if the mutation probability C is smaller or equal to the random generated number *ran*, then *SIV(i, h)* in H_i will be replaced with *SIV(j4, h)* in H_{j4} to finish the DELSS operation; finally, a new individual H_i is generated. From the above descriptions for the main updating procedures of BBO and BBOLS, it can be seen that the DELSS operation in BBOLS increases the diversity of the whole population by

Table 4
Pseudo-code of BBOLS.

BBOLS

1: Initialization
Initialize the BBOLS parameters: population size N, number of SIVs in an individual m, maximum number of generations Gen_{max}, maximum emigration rate E, maximum immigration rate I, elitism parameter $Keep$, and mutation rate probability C, and $gen = 0$.
Initialize the population: generate a random set of habitats P_0, and the population size is N.
2: Calculate the fitness value of each individual in P_0
3: Sort P_0 from best to worst according to the fitness value for each individual in P_0
4: Copy the first *Keep* individuals in the population and the corresponding fitness values for these individuals to *EliteSolution* and *EliteCost*, respectively
5: Map the fitness values to the number of species *S* in the population
6: Compute the immigration rate λ and emigration rate μ for each individual in the population
7: Migration
Modify the population by using migration based on local search operation as shown in Table 2, and place the newly generated population into *Island*.
8: Compute the fitness value for each individual in *Island*
9: Selection
Compare the fitness values for the individuals in *Island* with those for the corresponding individuals in the old population by employing the selection operation in Table 3, and select the individuals with higher fitness values to compose the new population to the next iteration.
10: Sort the newly generated population from best to worst
11: Copy the individuals in the *EliteSolution* which is generated in step (4), to the last *Keep* individuals in the population
12: Delete the reduplicative individuals in the population
13: Compute the fitness value for each individual in the population
14: Sort the population from best to worst
15: Stopping criteria
If $gen \geq Gen_{max}$ or an acceptable problem solution is found, then this loop can be terminated. Otherwise, if $gen = gen + 1$, proceed to step (4).

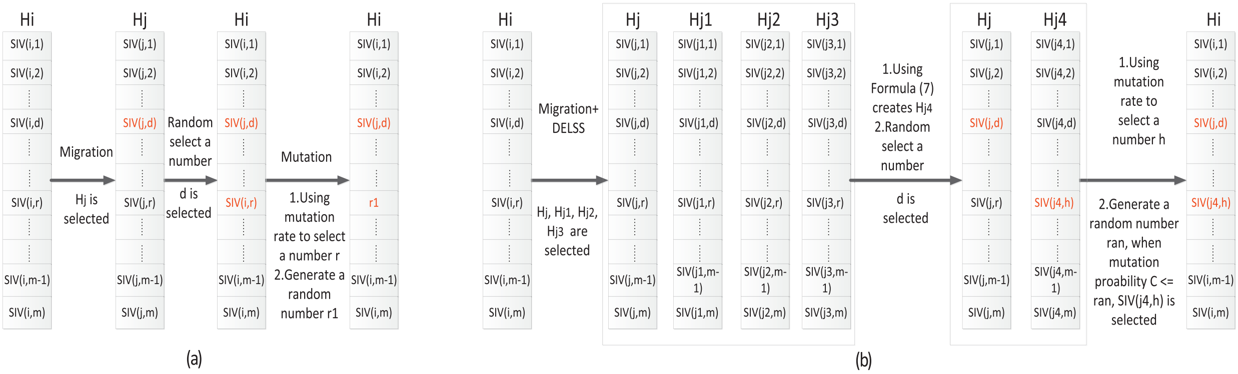

Fig. 2. (a) The main updating procedure of BBO (b) The main updating procedure of BBOLS.

selecting the other three individuals H_{j1}, H_{j2} and H_{j3} in the population which are used by Formula (7) to regenerate H_i so that making H_i jump out of the local optimal.

5. Simulation and analysis

In this section, using BBOLS to optimize the radiation beam patterns of LAAs and CAAs is simulated by using Matlab. Afterward, the results obtained by BBOLS are compared with those from BBO, FA and PSO. The experiments are performed on an Intel(R) Core(TM) 2 Duo CPU with 2.93 GHz and 3.00GB RAM.

5.1. Performance testing for BBO

In order to verify that BBO is suitable for the design of LAA and CAA, the testing results have been shown in Fig. 3(a) and Fig. 3(b), respectively. The experiment results are based on 20 independent tests for each case. It can be seen from Fig. 3(a) that with the increasing of the number of elements in LAA, BBO can get a lower maximum SLL than FA, PSO and the uniform case for each number of elements of the LAA. The similar results can be also found in Fig. 3(b) for CAA.

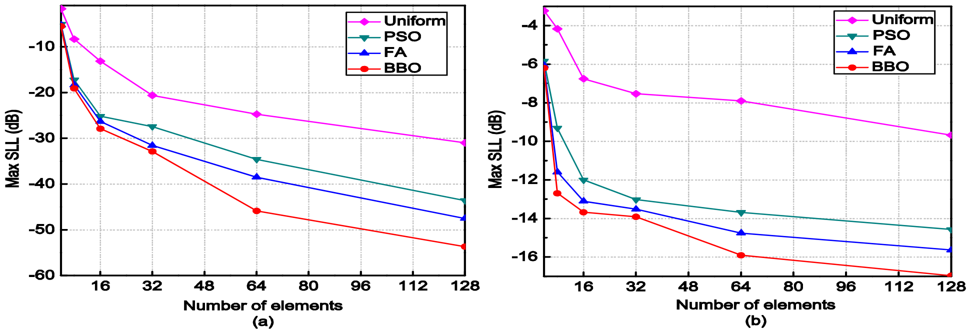

Fig. 3. (a) Performance testing of BBO for LAA (b) Performance testing of BBO for CAA.

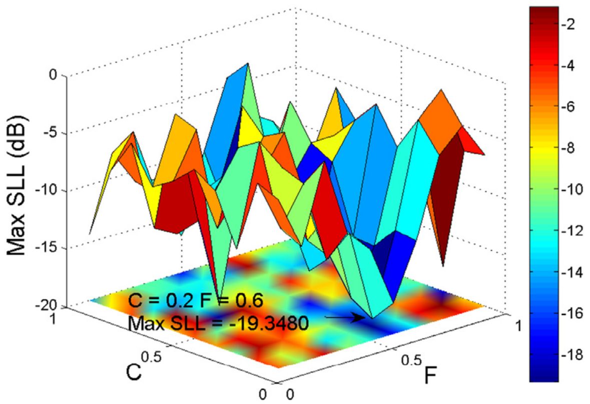

Fig. 4. Parameter sensitivity test for C and F in BBOLS.

Table 5
Parameter settings of BBOLS, BBO, FA, and PSO.

Parameter settings							
BBOLS	*popsize*: 100	Gen_{max}: 500	*pmutate*: 0.01	*I*: 1	*E*: 1	*C*: 0.2	*F*: 0.6
BBO	*popsize*: 100	Gen_{max}: 500	*pmutate*: 0.01	*I*: 1	*E*: 1		
FA	*popsize*: 100	Gen_{max}: 500	*LAC*: 1	*AC*: 0.2	*rp*: 0.25		
PSO	*popsize*: 100	Gen_{max}: 500	*CC*: 2	*SC*: 2			

5.2. Parameter selections of BBOLS

BBOLS has two new parameters C (Mutation probability) and F (Difference factor) compared with BBO. Fig. 4 shows the results of the parameter tuning procedure for C and F, the range of C is [0.1, 1], the range of F also is [0.1, 1], and each parameter is tested in a specific range with 2000 repetitions to get the optimal solution. It can be seen from Fig. 4 that the best values of C and F are $C=0.2$ and $F=0.6$. Table 5 shows the parameter settings of BBOLS algorithm and the other three benchmark algorithms.

5.3. Comparison of the improved factors of BBO

To verify the performance of the introduced improved factors, serial verification tests are constructed. The details of these tests are shown as follows.

5.3.1. Comparison of improved factors for LAA

Fig. 5(a) shows the convergence curves of the maximum SLL of the 8-element LAA obtained using BBO and BBO with DELSS. Fig. 5(b) shows the convergence curves of the maximum SLL of the 8-element LAA obtained using BBO and BBO with selection. Fig. 5(c) shows the convergence curves of the maximum SLL of the 32-element LAA obtained using BBO and BBO with DELSS. Fig. 5(d) shows the convergence curves of the maximum SLL of the 32-element LAA obtained using BBO and BBO with selection. For the 8-element LAA, given the very few elements for LAA and the symmetric placement of the eight elements, the algorithm only optimizes four elements for LAA. Therefore, the convergence rates of BBO with DELSS and BBO with selection are slightly better than that of BBO as shown in Figs. 5(a) and 5(b). However, for the 32-element LAA, given

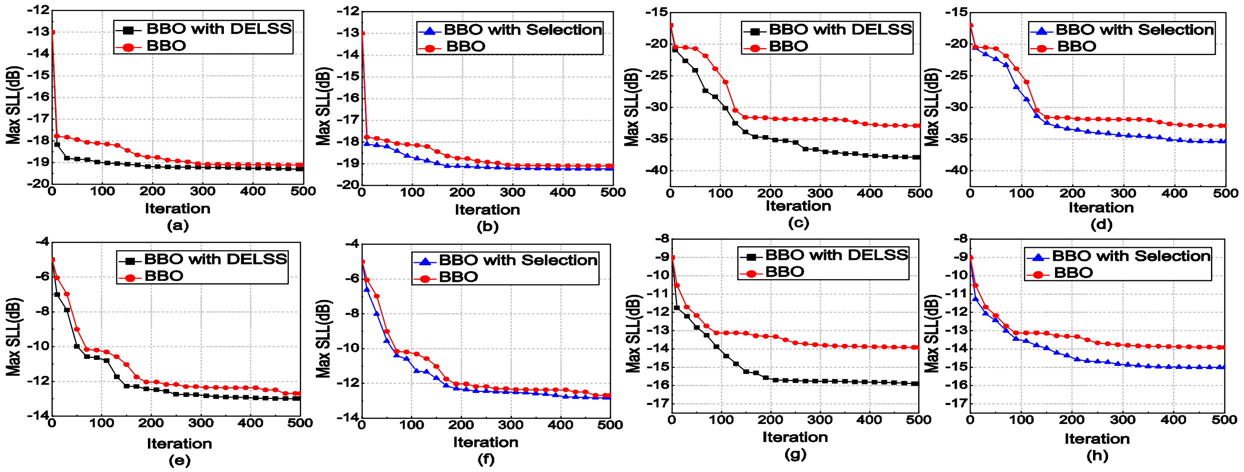

Fig. 5. Convergence rates for optimizing the beam patterns of LAA and CAA obtained using different methods. (a) Normal BBO and BBO with DELSS for $N=8$ LAA; (b) normal BBO and BBO with selection for $N=8$ LAA; (c) normal BBO and BBO with DELSS for $N=32$ LAA; and (d) normal BBO and BBO with selection for $N=32$ LAA; (e) Normal BBO and BBO with DELSS for $N=8$ CAA; (f) normal BBO and BBO with selection for $N=8$ CAA; (g) normal BBO and BBO with DELSS for $N=32$ CAA; and (h) normal BBO and BBO with selection for $N=32$ CAA.

Table 6
Excitation current values for the optimized 8-element LAA.

Algorithm	(I_1, I_2, I_3, I_4, I_5, I_6, I_7, I_8)	Max SLL(dB)
BBOLS	(0.4919, 0.5266, 0.7035, 0.7831, 0.7995, 0.6871, 0.5354, 0.4816)	−19.3480
BBO	(0.4618, 0.5675, 0.7120, 0.8918, 0.8167, 0.7693, 0.5607, 0.5806)	−19.1004
FA	(0.6389, 0.5840, 0.8841, 1.0000, 0.8252, 0.8798, 0.7151, 0.4618)	−18.3439
PSO	(0.8423, 0.5666, 1.0000, 1.0000, 0.9430, 0.8759, 0.7778, 0.2590)	−17.2310
Uniform	(1.0000, 1.0000, 1.0000, 1.0000. 1.0000, 1.0000, 1.0000, 1.0000)	−8.3097

the larger number of elements for LAA, the convergence rates of BBO with DELSS and BBO with selection are better than that of BBO as shown in Fig. 5(c) and (d). Given that DELSS is the major improved operation for BBOLS, the selection operation guarantees that the solutions from each iteration do not deviate far from the direction of the best solution. Therefore, the convergence rate of BBO with DELSS is better than that of BBO with selection.

5.3.2. Comparison of improved factors for CAA

Fig. 5(e) shows the convergence curves of the maximum SLL of the 8-element CAA obtained using BBO and BBO with DELSS. Fig. 5(f) shows the convergence curves of the maximum SLL of the 8-element CAA obtained using BBO and BBO with selection. Fig. 5(g) shows the convergence curves of the maximum SLL of the 32-element CAA obtained using BBO and BBO with DELSS. Fig. 5(h) shows the convergence curves of the maximum SLL of the 32-element CAA obtained using BBO and BBO with selection. For the 8-element CAA, the convergence rates of BBO with DELSS and BBO with selection are slightly better than that of BBO as shown in Fig. 5(e) and (f). For the 32-element CAA, the convergence rates of BBO with DELSS and BBO with selection are better than that of BBO as shown in Fig. 5(g) and (h). The convergence rate of BBO with DELSS is better than that of BBO with selection for CAA. These findings can be explained by the same reasons in Section 5.3.1.

5.4. Experiments on LAA

5.4.1. 8-element LAA

As shown in Table 6, the best solution obtained by using BBOLS is −19.3480 dB. "Best" refers to the solution that provides a radiation pattern with the lowest maximum SLL of the antenna array among all the tests. Moreover, the maximum SLLs obtained using BBO, FA, and PSO are −19.1004, −18.3439, and −17.2310 dB, respectively, and the maximum SLL for the uniform array is −8.3097 dB. Fig. 6(a) shows the radiation pattern obtained using BBOLS compared to those obtained using BBO, FA, and PSO. BBOLS obtains the minimum maximum SLL unlike the other three methods. To compare the convergence properties of BBOLS, BBO, FA, and PSO, Fig. 6(b) shows the convergence curves for achieving the maximum SLL of the 8-element LAA obtained using these algorithms. Fig. 6(b) clearly shows that the convergence rate of BBOLS is better than those of the other algorithms, and BBOLS obtains the lowest maximum SLL. Therefore, the simulation results for the 8-element LAA obtained using BBO and BBOLS are superior to those obtained using FA and PSO.

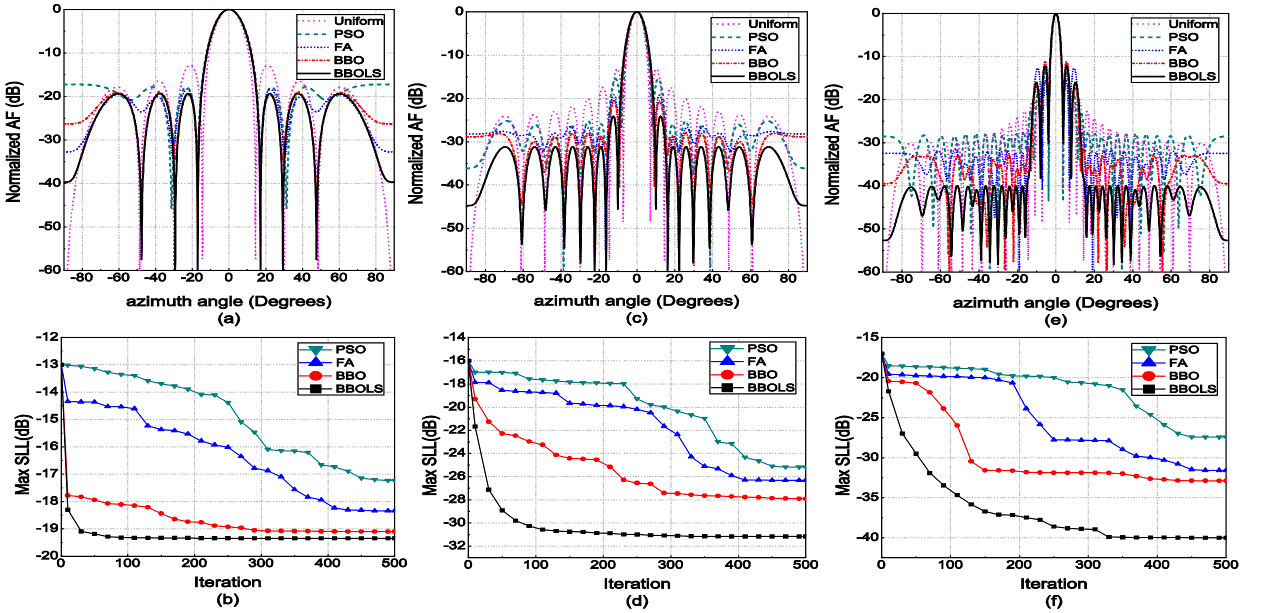

Fig. 6. (a) Radiation pattern of the optimized 8-element LAA; (b) Convergence curves of the optimized 8-element LAA; (c) Radiation pattern of the optimized 16-element LAA; (d) Convergence curves of the optimized 16-element LAA; (e) Radiation pattern of the optimized 32-element LAA; (f) Convergence curves of the optimized 32-element LAA.

Table 7
Excitation current values for the optimized 16-element LAA.

Algorithm	$(I_1, I_2, I_3, I_4, I_5, I_6, I_7, I_8, I_9, I_{10}, I_{11}, I_{12}, I_{13}, I_{14}, I_{15}, I_{16})$	Max SLL(dB)
BBOLS	(0.2912, 0.3576, 0.5247, 0.6522, 0.8063, 0.8931, 0.9614, 1.0000, 1.0000, 0.9784, 0.9145, 0.8054, 0.6955, 0.5154, 0.3657, 0.2933)	−31.1620
BBO	(0.3632, 0.3403, 0.5462, 0.6412, 0.8021, 0.8819, 0.9298, 0.8669, 0.9232, 0.8149, 0.8226, 0.7781, 0.6867, 0.5286, 0.4712, 0.3073)	−27.8963
FA	(0.2266, 0.2112, 0.3912, 0.4415, 0.5795, 0.4819, 0.6336, 0.6214, 0.5379, 0.6945, 0.6578, 0.5489, 0.4917, 0.4291, 0.3799, 0.1791)	−26.3008
PSO	(0.6015, 0.6733, 0.9039, 0.8248, 1.0000, 0.9557, 0.8729, 0.8938, 0.7917, 0.8644, 0.8440, 0.8226, 0.7826, 0.5914, 0.4420, 0.4205)	−25.1745
Uniform	(1.0000, 1.0000, 1.0000, 1.0000. 1.0000, 1.0000, 1.0000, 1.0000, 1.0000, 1.0000, 1.0000, 1.0000, 1.0000, 1.0000, 1.0000, 1.0000)	−13.1476

5.4.2. 16-element LAA

In this example, a 16-element LAA is optimized using BBOLS. Table 7 compares the best result obtained by using BBOLS with those obtained using BBO, FA, and PSO. The best maximum SLLs of the beam patterns obtained using BBOLS, BBO, FA, PSO, and uniform are −31.1620, −27.8963, −26.3008, −25.1745, and −13.1476 dB, respectively. Fig. 6(c) compares the radiation patterns obtained using BBOLS, BBO, FA, and PSO with a uniform LAA. The maximum SLL obtained by BBOLS is lower than those obtained using BBO, FA, and PSO. Fig. 6(d) shows the convergence rates of BBOLS, BBO, FA, and PSO. The convergence rate of BBOLS is better than those of the other three algorithms.

5.4.3. 32-element LAA

Similar with previous examples, Table 8 shows that the best maximum SLLs of the beam patterns obtained using BBOLS, BBO, FA, and PSO are −39.9888, −32.8789, −31.5828, and −27.4354 dB, respectively. The maximum SLL for the uniform array is −20.6184 dB. Fig. 6(e) compares the radiation patterns obtained using different optimization algorithms with a uniform array. The maximum SLL obtained using BBOLS is lower than those obtained using BBO, FA, and PSO. Fig. 6(f) shows the convergence curves during the optimization procedure of the 32-element LAA obtained using BBOLS, BBO, FA, and PSO. The convergence speed of BBOLS is faster than the other three methods. Therefore, the simulation results for the 32-element LAA obtained using BBOLS and BBO are superior to those obtained using FA and PSO.

Table 8
Excitation current values for the optimized 32-element LAA.

Algorithm	(I_1, I_2, I_3, I_4, I_5, I_6, I_7, I_8, I_9, I_{10}, I_{11}, I_{12}, I_{13}, I_{14}, I_{15}, I_{16}, I_{17}, I_{18}, I_{19}, I_{20}, I_{21}, I_{22}, I_{23}, I_{24}, I_{25}, I_{26}, I_{27}, I_{28}, I_{29}, I_{30}, I_{31}, I_{32})	Max SLL(dB)
BBOLS	(0.1817, 0.3002, 0.4569, 0.6488, 0.8278, 0.9570, 1.0000, 1.0000, 0.9652, 0.8441, 0.7756, 0.6987, 0.6917, 0.7401, 0.7844, 0.8480, 0.8637, 0.8487, 0.7681, 0.6827, 0.6312, 0.5725, 0.6285, 0.6995, 0.8279, 0.9368, 0.9597, 0.9272, 0.8123, 0.6443, 0.4241, 0.3040)	−39.9888
BBO	(0.3643, 0.2930, 0.5418, 0.6431, 0.8564, 0.9102, 0.8862, 0.7522, 0.7754, 0.6400, 0.5248, 0.5574, 0.4873, 0.5731, 0.5603, 0.7137, 0.7654, 0.7351, 0.7440, 0.7710, 0.7793, 0.7669, 0.7685, 0.8697, 0.8731, 0.9221, 0.9318, 0.8542, 0.7921, 0.6437, 0.4075, 0.1820)	−32.87893
FA	(0.4212, 0.5384, 0.6810, 0.7935, 0.8103, 0.6844, 0.5921, 0.5553, 0.4195, 0.3746, 0.5448, 0.5861, 0.9368, 0.8240, 1.0000, 0.9701, 0.9390, 0.8564, 0.7150, 0.5199, 0.5916, 0.6377, 0.6196, 0.7072, 0.7851, 0.9621, 0.7993, 0.7744, 0.7191, 0.5221, 0.3846, 0.1462)	−31.5828
PSO	(0.2633, 0.7693, 0.4023, 1.0000, 1.0000, 1.0000, 1.0000, 1.0000, 0.9969, 1.0000, 0.8908, 1.0000, 1.0000, 1.0000, 1.0000, 1.0000, 1.0000, 1.0000, 1.0000, 1.0000, 1.0000, 1.0000, 1.0000, 0.8837, 1.0000, 1.0000, 1.0000, 1.0000, 0.9772, 1.0000, 1.0000, 1.0000)	−27.4354
Uniform	(1.0000, 1.0000, 1.0000, 1.0000. 1.0000, 1.0000, 1.0000, 1.0000, 1.0000, 1.0000, 1.0000, 1.0000, 1.0000, 1.0000, 1.0000, 1.0000, 1.0000, 1.0000, 1.0000, 1.0000. 1.0000, 1.0000, 1.0000, 1.0000, 1.0000, 1.0000, 1.0000, 1.0000, 1.0000, 1.0000, 1.0000, 1.0000)	−20.6184

Table 9
Excitation current values for the optimized 8-element CAA.

Algorithm	(I_1, I_2, I_3, I_4, I_5, I_6, I_7, I_8) [d_1, d_2, d_3, d_4, d_5, d_6, d_7, d_8]	Max SLL(dB)
BBOLS	(0.6999, 0.5627, 0.1329, 0.9281, 1.0000, 0.4750, 0.7535, 0.4101) [0.3768, 0.7980, 0.4956, 0.3512, 0.6049, 0.8323, 0.7775, 0.3968]	−13.2098 $\rightarrow \Sigma = 4.6331$
BBO	(1.0000, 0.7354, 0.1136, 0.9105, 0.9361, 0.4828, 1.0000, 0.5896) [0.4032, 0.7482, 0.3452, 0.4879, 0.5963, 0.9124, 0.7414, 0.3819]	−12.6922 $\rightarrow \Sigma = 4.6165$
FA	(0.9401, 0.3614, 0.6308, 0.5315, 0.0412, 0.5637, 0.6257, 0.8609) [0.4721, 0.5369, 0.8659, 0.6201, 0.3483, 0.5770, 0.7442, 0.3648]	−11.5982 $\rightarrow \Sigma = 4.5293$
PSO	(0.7279, 0.6570, 0.0471, 0.7021, 0.9799, 0.5202, 0.3621, 1.0000) [0.9673, 0.2672, 0.4153, 1.0000, 0.5947, 1.0000, 0.6004, 1.0000]	-9.3150 $\rightarrow \Sigma = 5.8449$
Uniform	(1.0000, 1.0000, 1.0000, 1.0000. 1.0000, 1.0000, 1.0000, 1.0000) [0.5000, 0.5000, 0.5000, 0.5000, 0.5000, 0.5000, 0.5000, 0.5000]	-8.3097 $\rightarrow \Sigma = 4.0000$

5.5. Experiments on CAA

5.5.1. 8-element CAA

In this example, an 8-element CAA is optimized using BBOLS. As shown in Table 9, the lowest maximum SLL of the beam pattern obtained using BBOLS is −13.2098 dB. Moreover, the results obtained using BBO, FA, and PSO are −12.6922, −11.5982, and −9.3150 dB, respectively, and the best maximum SLL of the uniform array is −4.1702 dB. Fig. 7(a) shows the optimized radiation patterns of BBOLS, BBO, FA, and PSO. BBOLS can obtain the lowest maximum SLL compared with the other three methods. Fig. 7(b) shows the convergence curves during the optimization process obtained using BBOLS, BBO, FA, and PSO. The convergence rate of BBOLS is better than those of the other three algorithms.

5.5.2. 16-element CAA

Table 10 compares the best results of BBOLS, BBO, FA, and PSO in this example. The lowest maximum SLL of beam pattern obtained using BBOLS is −16.6733 dB, while those obtained using BBO, FA, PSO, and uniform are −13.6783, −13.1057, −12.0047, and −6.7578 dB, respectively. Fig. 7(c) compares the radiation patterns obtained using BBOLS, BBO, FA, and PSO with a uniform CAA. Fig. 7(c) shows that the maximum SLL obtained using BBOLS is lower than those obtained using BBO, FA, and PSO, while Fig. 7(d) shows the convergence curves obtained using these algorithms. The convergence rate of BBOLS is better than those of the other three algorithms, and the convergence rate of BBO is better than those of FA and PSO.

5.5.3. 32-element CAA

Similar to previous examples, Table 11 shows that the best maximum SLLs of the antenna array obtained using BBOLS, BBO, FA, and PSO are −16.5851, −13.9142, −13.5245, and −13.0242 dB, respectively. The maximum SLL for the uniform array is −7.5386 dB. Fig. 7(e) compares the radiation patterns those are obtained using the different optimization algorithms with a uniform array. The maximum SLL obtained using BBOLS is lower than those obtained using BBO, FA, and PSO. Fig. 7(f) shows the convergence rates for optimizing the 32-element CAA obtained by using BBOLS, BBO, FA, and PSO. BBOLS has a faster convergence speed than the other three methods. The simulation results for the 32-element CAA obtained using BBOLS and BBO are superior to those obtained using FA and PSO.

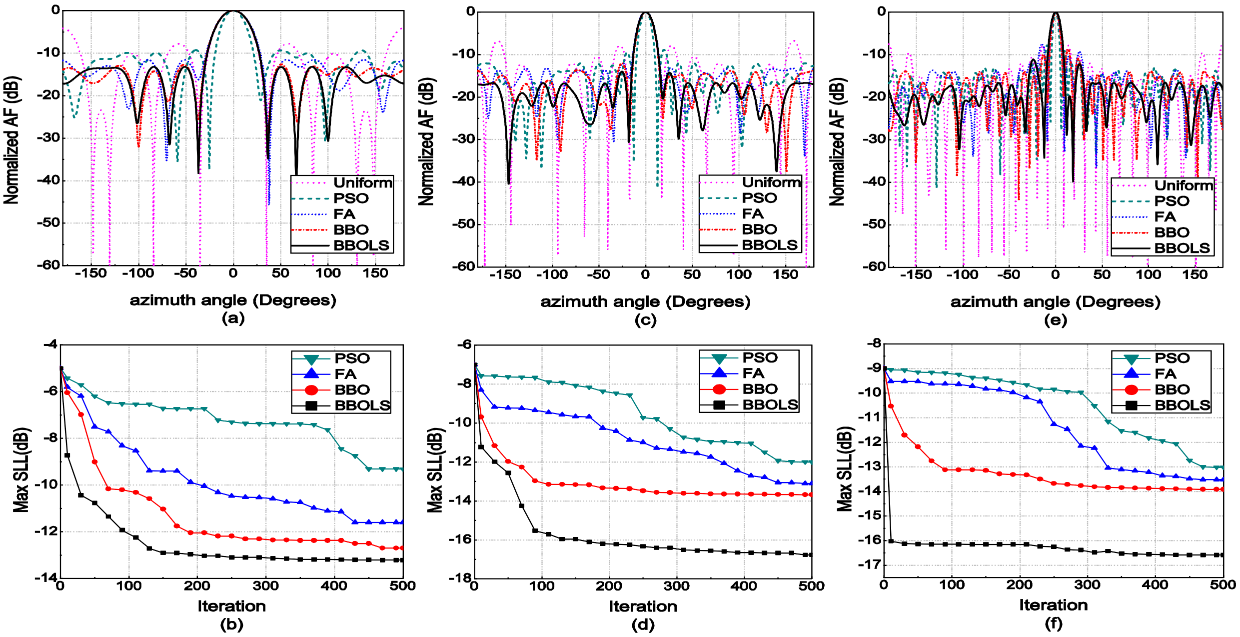

Fig. 7. (a) Radiation pattern of the optimized 8-element CAA; (b) Convergence curves of the optimized 8-element CAA; (c) Radiation pattern of the optimized 16-element CAA; (d) Convergence curves of the optimized 16-element CAA; (e) Radiation pattern of the optimized 32-element CAA; (f) Convergence curves of the optimized 32-element CAA.

Table 10
Excitation current values for the optimized 16-element CAA.

Algorithm	(I_1, I_2, I_3, I_4, I_5, I_6, I_7, I_8, I_9, I_{10}, I_{11}, I_{12}, I_{13}, I_{14}, I_{15}, I_{16}) [d_1, d_2, d_3, d_4, d_5, d_6, d_7, d_8, d_9, d_{10}, d_{11}, d_{12}, d_{13}, d_{14}, d_{15}, d_{16}]	Max SLL(dB)
BBOLS	(0.4900, 0.7323, 0.4765, 0.4390, 0.6680, 0.6880, 0.7747, 0.9177, 00.3393, 0.9270, 0.6050, 1.0000, 0.0000, 0.8899, 0.5803, 1.0000)	−16.6733
	[0.2879, 0.3763, 0.7940, 0.2188, 0.6158, 0.7753, 0.9366, 0.4024, 0.2159, 0.1930, 0.6429, 0.8678, 0.4550, 0.8128, 0.7882, 0.8747]	→ Σ = 9.2574
BBO	(1.0000, 0.9467, 1.0000, 0.8385, 0.4479, 0.2878, 1.0000, 1.0000, 1.0000, 0.0000, 1.0000, 0.6485, 0.5121, 0.9630, 0.5370, 0.6617)	−13.6783
	[0.2160, 0.4969, 0.8714, 0.7266, 0.8604, 1.0000, 0.2110, 0.3260, 0.3027, 0.3306, 0.7853, 0.8099, 0.4593, 0.2750, 1.0000, 0.5472]	→ Σ = 9.2183
FA	(0.4040, 0.6086, 0.8193, 0.4900, 0.3979, 0.2868, 0.7285, 0.0749, 0.2993, 0.3417, 0.7687, 0.1568, 0.1716, 0.3729, 0.0772, 1.0000)	−13.1057
	[0.3605, 0.3605, 0.3894, 0.9499, 0.9834, 0.5598, 0.6148, 0.2549, 0.2346, 0.9293, 0.8595, 0.1738, 0.9654, 0.5686, 0.1334, 0.4144]	→ Σ = 8.9218
PSO	(0.8369, 0.8178, 0.6699, 0.3570, 0.6544, 0.7847, 0.6969, 1.0000, 0.6378, 0.8504, 0.9100, 0.6323, 0.9926, 0.6807, 0.7901, 1.0000)	−12.0047
	[0.6605, 0.6575, 0.9638, 0.9469, 0.8070, 0.4662, 0.4663, 0.7198, 0.7576, 0.9315, 0.7098, 0.8096, 0.4483, 1.0000, 0.6191, 0.6697]	→ Σ = 11.6336
Uniform	(1.0000, 1.0000, 1.0000, 1.0000. 1.0000, 1.0000, 1.0000, 1.0000, 1.0000, 1.0000, 1.0000, 1.0000, 1.0000, 1.0000, 1.0000, 1.0000)	−6.7578
	[0.5000, 0.5000, 0.5000, 0.5000, 0.5000, 0.5000, 0.5000, 0.5000, 0.5000, 0.5000, 0.5000, 0.5000, 0.5000, 0.5000, 0.5000, 0.5000]	→ Σ = 8.0000

5.6. Electromagnetics (EM) simulation

In order to prove the performance of BBOLS that outperforms BBO, FA, PSO and the uniform case in practice conditions, an 8-element LAA for EM simulation has been designed based on HFSS 15.0. The physical structure of this antenna is shown in Fig. 8(a) in which $L = 40.49$ mm, $W = 48.40$ mm, $S_0 = 0.83$mmm, $S_1 = 3.4$ mm, $d = 6.12$ mm, the substrate layer is 1.575 mm Rogers RT/duroid 5880, the dielectric constant ε_r is 2.2, the frequency is 5 GHz, and the ground plane is modeled with copper and infinite lateral extends. The radiation beam patterns of this array with different excitation amplitudes obtained by BBOLS, BBO, FA, PSO, and the uniform case are shown in Fig. 8(b). The maximum SLLs of this antenna array obtained by using BBOLS, BBO, FA, PSO and uniform excitation in the EM simulation are −19.2631, −19.0001, −18.2013, −17.1274, and −7.9981. Therefore, the EM simulation results are similar with the simulation results. That is to say that BBOLS can still get the lower maximum SLL than BBO, FA, and PSO for real-world antenna array.

Table 11
Excitation current values for the optimized 32-element CAA.

Algorithm	$(I_1, I_2, I_3, I_4, I_5, I_6, I_7, I_8, I_9, I_{10}, I_{11}, I_{12}, I_{13}, I_{14}, I_{15}, I_{16}, I_{17}, I_{18}, I_{19}, I_{20}, I_{21}, I_{22}, I_{23}, I_{24}, I_{25}, I_{26}, I_{27}, I_{28}, I_{29}, I_{30}, I_{31}, I_{32})$ $[d_1, d_2, d_3, d_4, d_5, d_6, d_7, d_8, d_9, d_{10}, d_{11}, d_{12}, d_{13}, d_{14}, d_{15}, d_{16}, d_{17}, d_{18}, d_{19}, d_{20}, d_{21}, d_{22}, d_{23}, d_{24}, d_{25}, d_{26}, d_{27}, d_{28}, d_{29}, d_{30}, d_{31}, d_{32}]$	Max SLL(dB)
BBOLS	(1.0000, 0.6348, 0.5527, 0.9406, 0.6882, 0.6822, 0.8181, 0.0000, 0.5327, 0.7516, 0.5257, 0.0000, 1.0000, 0.6921, 0.8792, 0.6809, 1.0000, 0.7360, 0.2451, 0.0460, 0.4198, 0.0647, 0.0222, 0.4325, 0.0000, 1.0000, 0.7245, 0.9801, 0.6404, 0.6677, 0.7406, 1.0000)	−16.5851
	[0.5413, 0.1150, 0.4336, 1.0000, 0.9209, 0.3582, 0.7552, 0.0000, 0.3005, 0.3396, 0.9425, 0.2535, 0.8397, 0.3466, 0.2834, 0.2001, 0.3262, 0.3780, 0.5032, 0.8390, 0.8097, 0.0772, 0.3655, 0.3410, 0.3105, 0.9674, 0.7964, 0.8348, 0.3030, 0.3609, 0.1493, 0.4557]	$\rightarrow \Sigma = 15.4479$
BBO	(0.8647, 1.0000, 0.6054, 0.3098, 1.0000, 0.6845, 1.0000, 0.4775, 1.0000, 0.6959, 0.5825, 1.0000, 0.9601, 1.0000, 1.0000, 0.4661, 0.7870, 0.2630, 0.2211, 0.9318, 0.7730, 0.3716, 0.5146, 0.9099, 0.0000, 1.0000, 1.0000, 0.7552, 1.0000, 0.4922, 0.3608, 0.6200)	−13.9142
	[0.5730, 0.4293, 0.2670, 0.8739, 0.6665, 0.2742, 0.4172, 1.0000, 0.8116, 0.3299, 0.8512, 0.3726, 0.4149, 0.4632, 0.4938, 0.1964, 0.5497, 0.4101, 0.6471, 0.1288, 0.6822, 0.3962, 0.8517, 0.8044, 0.2874, 1.0000, 0.9396, 0.4489, 0.5323, 0.4450, 0.4320, 0.5474]	$\rightarrow \Sigma = 17.5375$
FA	(0.8835, 0.9907, 0.5038, 0.4758, 0.6685, 0.0068, 0.4451, 0.4837, 0.3490, 0.5328, 0.4048, 0.3528, 0.3790, 0.6402, 0.6336, 0.6758, 0.5588, 0.6602, 0.9754, 0.3376, 0.7330, 0.5222, 0.6572, 0.5459, 0.7848, 0.5566, 0.8254, 0.3162, 0.4849, 0.3710, 0.3988, 0.3887)	−13.5245
	[0.3952, 0.4453, 0.2059, 0.4122, 0.4190, 0.3475, 0.7074, 0.2898, 0.5072, 0.5350, 0.7330, 0.5438, 0.3788, 0.3542, 0.7348, 0.4804, 0.6563, 0.3937, 0.4550, 0.3926, 0.6195, 0.3694, 0.4959, 0.4397, 0.6503, 0.2136, 0.3425, 0.2574, 0.7814, 0.8810, 0.3090, 0.8262]	$\rightarrow \Sigma = 15.5730$
PSO	(1.0000, 0.8819, 0.8969, 0.9854, 0.9999, 0.8341, 0.8465, 0.2566, 0.9988, 0.6656, 0.8267, 0.1790, 0.9021, 0.7454, 1.0000, 0.8065, 0.7017, 1.0000, 0.7662, 0.7831, 0.9158, 0.9998, 0.7184, 0.9556, 0.8285, 0.5407, 1.0000, 0.9997, 0.6698, 0.9750, 0.2969, 0.0000)	−13.0242
	[0.1423, 0.6427, 0.7283, 0.3905, 0.9932, 0.9999, 0.9928, 0.8365, 0.9101, 0.8615, 0.7504, 0.9939, 0.6947, 0.4440, 0.9820, 0.6330, 0.7791, 0.9082, 0.2304, 0.2335, 0.9973, 0.9998, 0.8646, 0.3421, 0.6645, 0.9984, 0.3306, 0.8308, 0.9670, 0.9451, 0.9960, 0.9438]	$\rightarrow \Sigma = 24.0270$
Uniform	(1.0000, 1.0000, 1.0000, 1.0000. 1.0000, 1.0000, 1.0000, 1.0000, 1.0000, 1.0000, 1.0000, 1.0000, 1.0000, 1.0000, 1.0000, 1.0000, 1.0000, 1.0000, 1.0000, 1.0000. 1.0000, 1.0000, 1.0000, 1.0000, 1.0000, 1.0000, 1.0000, 1.0000, 1.0000, 1.0000, 1.0000, 1.0000)	−7.5386
	[0.5000, 0.5000]	$\rightarrow \Sigma = 16.0000$

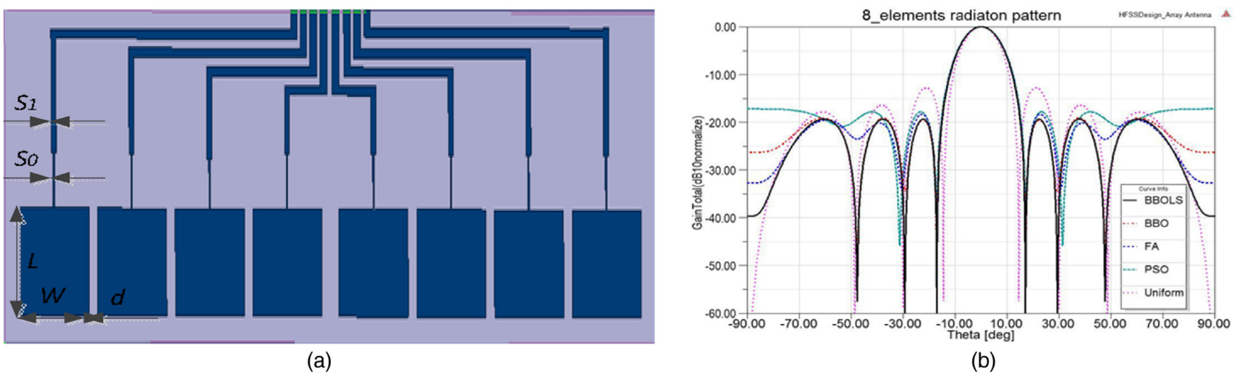

Fig. 8. (a) Physical structure of the micro-strip patch antenna array; (b) Normalized gain pattern of the real-world antenna array.

6. Conclusion

A novel optimization algorithm called BBOLS is proposed to model the design of LAAs and CAAs for reducing the maximum SLLs. BBOLS efficiently computes an optimal set of excitation currents values for LAA and an optimal set of excitation current and spacing values for CAA. The improved DELSS and selection operators in BBOLS efficiently improve the convergence rate, prevent solutions from being trapped into the local optimum, and guarantee that the solutions from each iteration will go to the direction of the final best solution. The effectiveness of these improved operators is verified by simulations. Moreover, simulation results reveal that the proposed BBOLS algorithm outperforms the normal BBO, FA, PSO, and a uniform case for both the design of LAAs and CAAs. In addition, an EM simulation by using HFSS 15.0 is also implemented to verify the effectiveness of BBOLS to imitate the realistic condition. The results indicate that BBOLS still can get a better performance than the normal BBO, FA, PSO and a uniform case in the practice conditions. Therefore, BBOLS is suitable for solving optimization problems in electromagnetics, and can be also extended to optimize other antenna arrays. However, this paper only considered suppressing the sidelobe levels of LAAs and CAAs. Thus, decreasing the noise sensitivity, reducing the robustness or input impedance of antenna arrays to the required level will be taking into account in our future work.

Acknowledgments

We thank the anonymous referees for their valuable suggestions and comments. We thank Prof. Ying Zhang, Georgia Institute of Technology, USA, for her carefully English review of this paper. This work was supported by the National Nature Science Foundation of China (Grant Nos. 61073164 and 61373123), the Fund of Key Laboratory of Symbolic Computation and Knowledge Engineering of Ministry of Education (93K172012K05), the Key Development Program for Science and Technology of Jilin Province, China (Grant No. 20150414004GH) and Chinese Scholarship Council (No. [2016] 3100).

Reference

[1] Alreshaid AT, Sharawi MS, Podilchak S, Sarabandi K. Compact millimeter-wave switched-beam antenna arrays for short range communications. Microwave Opt Technol Lett 2016;58.8:1917–21.
[2] Chen M, Zhang Y, Li Y, Mao S. EMC: Emotion-aware mobile cloud computing in 5 G. Netw IEEE 2015;29.2:32–8.
[3] Ge X, Tu S, Mao G, Wang CX. 5 G Ultra-Dense Cellular Networks. IEEE Wirel Commun 2015;23.1:72–9.
[4] Reyna A, Panduro MA, Rio-Bocio CD, Méndez AL. Design of different planar geometries of antenna arrays for isoflux radiation in GEO satellites. Telecommun Syst 2016:1–11.
[5] Yahya R-S, Densmore AC. Technology trends and challenges of antennas for satellite communication systems. IEEE Trans Anten Propagation 2015;63.4:1191–204.
[6] Zhang W, Li L, Li F. Reducing the number of elements in linear and planar antenna arrays with sparseness constrained optimization. Anten Propagation IEEE Trans 2011;59.8:3106–11.
[7] Zhang Z, Li T, Yuan F, Yin L. Synthesis of linear antenna array using genetic algorithm to control side lobe level. In: Computer engineering and networking. Springer International Publishing; 2014. p. 39–46.
[8] Florence VP, S N R G. Synthesis of linear antenna arrays using accelerated particle swarm optimization algorithm. Int J Comput Appl 2014;103.3:43–9.
[9] Singh U, Rattan M. Design of linear and circular antenna arrays using cuckoo optimization algorithm. Progr Electromag Res C 2014;46:1–11.
[10] Lakshman P, Ghosh D. Linear antenna array synthesis using cat swarm optimization. AEU - Int J Electr Commun 2014;68.6:540–9.
[11] Swain P, Mohanty SK, Mangaraj BB. Linear dipole antenna array design and optimization using gravitational search algorithm. International conference on advances in electrical, electronics, information, communication and bio-informatics IEEE; 2016.
[12] Qubati GM, Dib NI. Microstrip patch antenna optimization using modified central force optimization. Pier B 2010.
[13] Guney K, Onay M. Synthesis of thinned linear antenna arrays using bees algorithm. Microwave Opt Technol Lett 2011;53.4:795–9.
[14] Ram G, Mandal D, Kar R, Ghoshal SP. Design of non-uniform circular antenna arrays using firefly algorithm for side lobe level reduction. Waset Org 2014;8.1:36–41.
[15] Balanis CA. Antenna theory: analysis and design. 3rd ed; 2012.
[16] Sharaqa A, Dib N. Design of linear and elliptical antenna arrays using biogeography based optimization. Arab J Sci Eng 2014;39.4:2929–39.
[17] Simon D. Biogeography-based optimization. IEEE Trans Evol Comput 2009;12.6:702–13.
[18] Ying Q, Gao YL, Jiang QY. Differential evolutionary algorithm with a new local search strategy. J Taiyuan Univ Technol 2011.

Han Li received the BS degree in Software Engineering from Jilin University, China, in 2015, and is currently a master student in College of Computer Science and Technology at Jilin University. Her research interest is the design of array antennas.

Yanheng Liu received MSc and PhD degrees in computer science from Jilin University, China. He is currently a professor in Jilin University, China. His primary research interests are in network security, network management, mobile computing network theory and applications, etc.

Geng Sun received BS degree in Communication Engineering from Dalian Polytechnic University, China in 2011. He is currently a PhD candidate in College of Computer Science and Technology at Jilin University, and a visiting researcher at Georgia Institute of Technology, USA. His research interests include wireless sensor networks and collaborative beamforming.

Aimin Wang received PhD degree in Communication and Information System from Jilin University. He is currently an associate professor at Jilin University. His research interests are wireless sensor networks and QoS for multimedia transmission.

Shuang Liang received BS degree in Communication Engineering from Dalian Polytechnic University, China, in 2011. She is currently studying Software Engineering at Jilin University to get MS degree. Her research interests focus on wireless communication and design of array antennas.